Stresses and Strains in Thick Perforated Orthotropic Plates

A. Alshaya[1]; J. Hunt[2]; and R. Rowlands[3]

Abstract: Stress and strain concentrations and in-plane and out-of-plane stress constraint factors associated with a circular hole in thick, loaded orthotropic composite plates are determined by three-dimensional finite element method. The plate has essentially infinite in-plane geometry but finite thickness. Results for Sitka spruce wood are emphasized, although some for carbon-epoxy composites are included. While some results are similar to those for isotropy, there are significant consequences due to material orthotropy. Maximum stress and strain concentration factors occur at midplane for thin plates but closer to the external traction-free surfaces for thick plates. These factors decrease as the plate surface is approached and reach lower values unrepresentative of the maximum values. Differences between the midplane and/or maximum and surface stress or strain concentration factors in Sitka spruce, range from 8% if the wood grain is parallel to the vertically applied load to 15% when the grain is perpendicular to the load. These values exceed those typically reported for isotropic materials. Stress and strain concentration factors tend to differ in magnitude from each other. The combination of high local stresses and directional strength dependency of orthotropic materials can be particularly important. That maximum stress and/or strain concentrations in thick plates occur on other than the external plate surfaces where they are most readily measured is technically significant. The E_{11}/E_{22} ratio in Sitka Spruce exceeds that in the carbon composite by 60%. However, when loading parallel to the strong/stiff directions, the plane-stress tensile stress concentration factors of the two materials are comparable to each other. **DOI: [10.1061/(ASCE)EM.1943-7889.0001138](#).** © *2016 American Society of Civil Engineers.*

Author keywords: Holes; Thick plates; Three-dimensional stresses; Three-dimensional strains; Constraint factors; Orthotropy; Sitka Spruce; Carbon/epoxy composite.

Introduction

Engineering components often involve holes or notches and an assessment of the structural reliability necessitates knowing the stresses and the strains associated with such geometric discontinuities. Round holes are common, and their accompanying stresses and strains can reduce mechanical performance. Such stress/strain risers can precipitate cracks, thereby aggravating the situation (Broek 1987).

Stress concentration factors are available for many plane-stress isotropic cases (Timoshenko and Goodier 1970; Pilkey and Pilkey 2008; Young and Budynas 2002). Plane solutions are valid for plates having vanishing thickness (plane-stress) compared to the size of any cutouts or for infinite thickness (plain-strain). Notwithstanding the technical importance, few theoretical/analytical three-dimensional (3D) solutions exist for nontrivial geometries or loading conditions.

Using a modified Ritz method, Sternberg and Sadowsky (1949) obtained an approximate solution for the three-dimensional stress distribution for a circular hole in a uniaxially loaded, infinite isotropic plate having arbitrary thickness. They showed that for a plate thickness 0.7 times the radius of the hole, the maximum stress concentration at the traction-free surface is 7% less, whereas that at mid-plane is 3% higher, than the plane-stress value. Youngdal and Sternberg (1966) subsequently found that for an infinitely thick component subjected to shear, the maximum stress at the surface of the hole is 23% less, and that at the depth equal to the hole radius is 3% higher, than that for a thin component. Folias (1975, 1987) and Folias and Wang (1990) demonstrated that the stress concentration factor in a circularly perforated three-dimensional elastic plate is sensitive to the plate thickness and Poisson's ratio. The condition starts to change from plane-stress to plane-strain when the ratio of hole radius to plate thickness is 0.5. When this ratio is less than 0.5, the maximum stress concentration factor occurs at the midplane, and when this ratio exceeds 0.5, the maximum stress concentration factor occurs close to the external traction-free surfaces. Based on the generalized plane-strain assumption that the out-of-plane strain is a constant, Kotousov and Wang (2002a, b, c) and Kotousov and Tan (2004) provided an analytical solution for the three-dimensional stress distribution in an isotropic perforated plate having arbitrary thickness. They considered the effects of Poisson's ratio and plate thickness on the in-plane stress concentration factor and the out-of-plane stress constraint factor. Dai and Gong (2013), by also assuming the out-of-plane strain in the thickness direction is a constant, obtained a theoretical solution for the three-dimensional stresses in an infinite isotropic elastic plate perforated with a circular hole. Their results show differences between the three-dimensional and plane-stress solutions, a significant effect of the Poisson's ratio on the tangential stress near the surface of the hole, and the effects of the plate thickness and Poisson's ratio on the stress concentration and the out-of-plane constraint factors. Yang et al. (2008) studied the coupled influence of Poisson's ratio and plate thickness on the stress and strain

[1]Graduate Student, Univ. of Wisconsin-Madison, Madison, WI 53706. E-mail: alshaya@wisc.edu

[2]Research Mechanical Engineer, USDA Forest Products Laboratory, Madison, WI 53726. E-mail: jfhunt@fs.fed.us

[3]Professor, Univ. of Wisconsin-Madison, Madison, WI 53706 (corresponding author). E-mail: rowlands@engr.wisc.edu

concentration factors using finite element method (FEM). The magnitude of their stress and strain concentration factors differ.

The previously discussed analyses are for isotropic materials. While extensive acceptance and use of orthotropic composite structures require confidence in their load carrying capacity, the authors are unaware of prior publications addressing the 3D stress or strain concentrations associated with geometric discontinuities in thick orthotropic plates. The fact that orthotropic materials can produce extremely high stress concentrations compared with isotropic materials motivates the need to know the stresses in orthotropic/composite structures containing holes or notches, including when the thickness is large compared with the size of the discontinuities.

The present research considers the 3D stress and strain concentrations, and the in-plane and out-of-plane stress constraint factors, in a large, uniaxially loaded, thick orthotropic plate containing a circular hole. Although the behavior in Sitka spruce wood is emphasized since this is a commonly employed and highly orthotropic ($E_{11}/E_{22} = 23$) structural material, some results for a unidirectional carbon/epoxy composite ($E_{11}/E_{22} = 14$) are included to illustrate the consequences of variations in orthotropy. Of structural relevance, Rhee et al. (2012) showed that the effect of stress concentrations on strength in artificial composites can be appreciably different than in natural orthotropic materials such as wood. The situations at the edge of the hole are studied as a function of changes in plate thickness and orthotropic directions. Where possible, the present results are correlated with available information.

Problem Definition

Geometry and Loading

A large, finite thickness homogeneous elastic plate containing a hole of radius a is subjected to far-field vertical tensile stress, σ, has a height $2H$, width $2W$ and thickness $2L$ as shown in Fig. 1. The origin of the xyz coordinate system is located at the middle of the plate (and center of the hole). The plane $z = 0$ is at the midplane of the plate, and the plate has external traction-free vertical surfaces at $z = \pm L$. The half-width, W, and half-height, H, of the plate are taken to be 100 times the radius of the hole, i.e., $W/a = H/a = 100$. The normalized half-thickness of the plate L/a is varied from 0.1 (plane stress condition) to 10.

Stresses and Strains

The stress and strain concentration factors at the edge of the hole in vertical planes of $x = a$, $y = 0$ and $-L \leq z \leq L$ in Fig. 1 are defined as

$$K^{\sigma} = \frac{\sigma_{yy}(a,0,z)}{\sigma_{\text{net}}}, \qquad K^{\varepsilon} = \frac{\varepsilon_{yy}(a,0,z)}{\varepsilon_{\text{net}}} \qquad (1)$$

where $\sigma_{\text{net}} = \sigma A/A_{\text{net}}$ and $\varepsilon_{\text{net}} = \sigma A/EA_{\text{net}}$ are the nominal stress and strain at the net section of the plate; A = gross area, i.e., $A = (2L)(2W)$ and the net area $A_{\text{net}} = (2W - 2a)(2L)$. The maximum stress and strain concentration factors occurring along the z-axis at $x = a$ and $y = 0$ are denoted by $K^{\sigma}_{\max}$ and $K^{\varepsilon}_{\max}$, respectively. The values of K^{σ} and K^{ε} at $x = a$, $y = 0$ and $z = 0$ (at the midplane) are denoted by K^{σ}_{mp} and $K^{\varepsilon}_{\text{mp}}$. The corresponding values of K^{σ} and K^{ε} on the external traction-free surfaces of the plate ($x = a$, $y = 0$, and $z = \pm L$) are denoted by K^{σ}_{sur} and $K^{\varepsilon}_{\text{sur}}$, i.e.,

$$K^{\sigma}_{\max} = \max_{0 \leq z \leq L} \frac{\sigma_{yy}(a,0,z)}{\sigma_{\text{net}}}, \qquad K^{\varepsilon}_{\max} = \max_{0 \leq z \leq L} \frac{\varepsilon_{yy}(a,0,z)}{\varepsilon_{\text{net}}} \qquad (2)$$
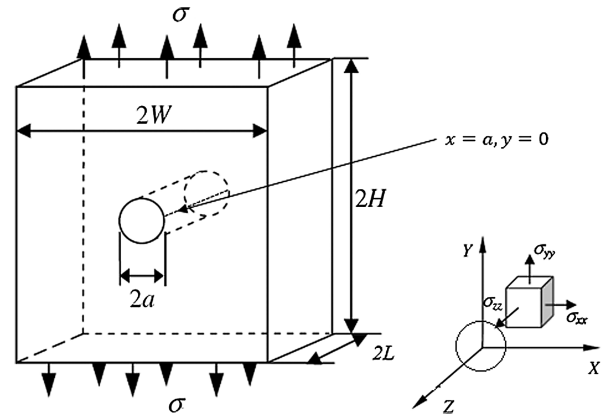

Fig. 1. Plate geometry and coordinate system

$$K^{\sigma}_{\text{mp}} = \frac{\sigma_{yy}(a,0,0)}{\sigma_{\text{net}}}, \qquad K^{\varepsilon}_{\text{mp}} = \frac{\varepsilon_{yy}(a,0,0)}{\varepsilon_{\text{net}}} \qquad (3)$$

$$K^{\sigma}_{\text{sur}} = \frac{\sigma_{yy}(a,0,\pm L)}{\sigma_{\text{net}}} \cdot K^{\varepsilon}_{\text{sur}} = \frac{\varepsilon_{yy}(a,0,\pm L)}{\varepsilon_{\text{net}}} \qquad (4)$$

The stress and strain concentration factors for plane-stress condition are represented by K^{σ}_{ps} and $K^{\varepsilon}_{\text{ps}}$, respectively. For a plane-stress, perforated infinite orthotropic plate subjected to a unidirectional tensile stress σ parallel to the y-axis, the in-plane vertical stress distribution solution at $y = 0$ in the vicinity of the edge of the hole is (Lekhnitskii 1969)

$$\frac{\sigma_{yy}(x,0)}{\sigma} = 1 + \text{Re}\left\{ \frac{1}{\beta - \delta} \left[\frac{-\delta(1 - i\beta)}{\sqrt{\zeta^2 - 1 - \beta^2}(\zeta + \sqrt{\zeta^2 - 1 - \beta^2})} \right. \right.$$
$$\left. \left. + \frac{-\beta(1 - i\delta)}{\sqrt{\zeta^2 - 1 - \delta^2}(\zeta + \sqrt{\zeta^2 - 1 - \delta^2})} \right] \right\} \qquad (5)$$

where β and δ = imaginary parts of the complex material properties and $\xi = x/a$ such that $\zeta \geq 1$. For an elastic orthotropic material in three dimensions, ε_{yy} can be evaluated from Hooke's law as (Daniel and Ishai 2006)

$$\varepsilon_{yy} = \frac{\sigma_{yy}}{E_y} - \frac{\nu_{xy}}{E_x}\sigma_{xx} - \frac{\nu_{zy}}{E_z}\sigma_{zz} = \frac{\sigma_{yy}}{E_y}\left(1 - \frac{\nu_{yx}\sigma_{xx}}{\sigma_{yy}} - \frac{\nu_{yz}\sigma_{zz}}{\sigma_{yy}}\right) \qquad (6)$$

Dividing Eq. (6) by ε_{net}, rearranging and setting $\sigma_{\text{net}} = E_y\varepsilon_{\text{net}}$, the following expression can be obtained:

$$K^{\varepsilon} = K^{\sigma}(1 - \nu_{yx}T_x - \nu_{yz}T_z - \nu_{yz}T_x \cdot T_z) \qquad (7)$$

where $T_z = \sigma_{zz}/(\sigma_{xx} + \sigma_{yy})$ is the out-of-plane stress constraint factor; and $T_x = \sigma_{xx}/\sigma_{yy}$ is the in-plane stress constraint factor. For a finite thickness orthotropic plate, the ratio of stress and strain concentration factors, $K^{\varepsilon}/K^{\sigma}$, is a function of Poisson's ratios ν_{yx} and ν_{yz} and the in-plane, T_x, and out-of-plane, T_z, stress constraint factors [Eq. (7)]. Note that $T_x = 0$ at $(a,0,z)$ for all z and $T_z = 0$ at the external traction-free surface $(x,0,\pm L)$.

Sitka Spruce Properties

The Sitka spruce constitutive properties employed are those of Table 1. The xy-plane of the orthotropic wood plate is in the longitudinal (grain orientation) and tangential plane of the wood and the axis of the hole is parallel to the radial direction of the wood or z-direction (Fig. 1).

Table 1. Constitutive Properties of the Sitka Spruce Wood (Data from Wood Handbook 1999)

Property	Value
Elastic moduli (MPa)	
E_L	11,450
E_T	492
E_R	893
Shear moduli (MPa)	
G_{LT}	698
G_{TR}	34.4
G_{RL}	733
Poisson's ratios	
ν_{LT}	0.47
ν_{TR}	0.25
ν_{RL}	0.04
ν_{TL}	0.025
ν_{RT}	0.46
ν_{LR}	0.37

Note: L, T, and R denote longitudinal, tangential, and radial directions of the wood.

Finite Element Model

Due to symmetry, only one-eighth of the plate was modeled. The FEM used *ANSYS* eight-node solid linear elements (Solid185). Mapped meshing utilized 20 planar layers through the thickness of the plate. The distance between each of these layers was fixed and the in-plane size of the elements decreased as one approached the hole. Because of the limited number of nodes allowed by *ANSYS*, this mesh was too coarse to produce satisfactory results in the region of the hole. A submodeling approach (also known as the cut-boundary displacement method) was subsequently employed. By creating a finer mesh near the hole and applying submodeling based on St. Venant's principle, more reliable results were obtained. However, accuracy necessitates the boundaries of the submodel be sufficiently far from the hole. The one-eighth submodel had 25,000 elements and 27,716 nodes. This technique was validated by comparing the numerically predicted variation of the stress $\sigma_{yy}(x, 0, z)$, normalized by far-field stress, σ, on different plane layers z/L parallel to the midplane for normalized thickness $L/a = 5$ with two-dimensional (2D) finite element analysis (Alshaya 2016) and plane-stress distribution of Eq. (5) for $x/a \geq 1$ shown in Fig. 2.

For the 3D state of stress around a circular hole of radius a in an isotropic plate of thickness $2L$ subjected to a unidirectional tensile stress σ parallel to the y-axis, Sternberg and Sadowsky (1949) determined the radial, σ_{rr}, tangential, $\sigma_{\theta\theta}$ and axial, σ_{zz} stresses in the vicinity of the edge of the hole to be

$$\sigma_{rr} = \frac{1}{2}\left(1 - \frac{1}{\rho^2}\right) + \frac{1}{2}\left(1 - \frac{4}{\rho^2} + \frac{3}{\rho^4}\right)\cos 2\theta$$
$$+ \frac{1}{2\Delta^2}\bar{Z}_n'' \cos 2\theta \sum_{i=1}^{2} L\frac{\lambda_{1i}}{\rho^{q+i}} \qquad (8)$$

$$\sigma_{\theta\theta} = \frac{1}{2}\left(1 + \frac{1}{\rho^2}\right) - \frac{1}{2}\left(1 + \frac{3}{\rho^4}\right)\cos 2\theta$$
$$+ \frac{1}{2\Delta^2}\bar{Z}_n'' \cos 2\theta \sum_{i=1}^{2}\frac{1}{\rho^{q+i}}\{[-(q+i-1)L+1]\lambda_{1i}$$
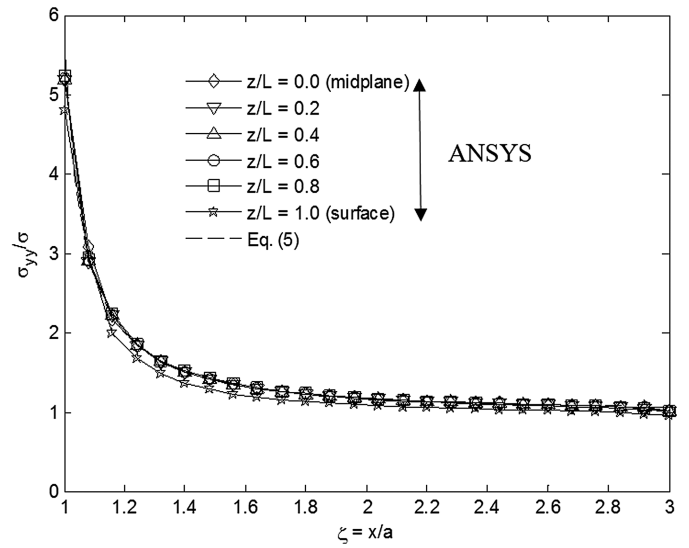$$+ L(\lambda_{2i} + 2\lambda_{3i})\} \qquad (9)$$

Fig. 2. Stress distribution, $\sigma_{yy}(x, 0, z)/\sigma$, for $x/a \geq 1$ on different planes, z/L, for thickness $L/a = 5$ in Sitka spruce when longitudinal axis (grain orientation, L-direction) is parallel to the applied vertical stress, σ

$$\frac{\sigma_{zz}}{\cos 2\theta} = \frac{1}{2}\bar{Z}_n \sum_{i=1}^{2}\frac{1}{\rho^{q+i+2}}\{[4(1+i-1)L-4]\lambda_{1i}$$
$$+ [(1+i-4)L-1]\lambda_{2i} + [-2(q+i+2)L+2]\lambda_{3i}\} \qquad (10)$$

where $\rho = r/a$ are dimensionless cylindrical coordinates; $\Delta = L/a$ is thickness ratio; $\bar{Z}_n = \bar{Z}_n(\xi) = \Delta^4(\xi^n - 1)^2$ and $\bar{Z}_n''$ are the second derivative with respect to $\xi = z/L$, $L(r) = \ln r$; and the exponents n, q as well as the values of $\lambda_{\alpha i}$ ($\alpha = 1, 2, 3$; $i = 1, 2$) are parameters that depend on Δ and ν. When $\Delta \to 0$, the equations reduced to plane-stress. At the midplane, i.e., $\xi = 0$, the last term also vanishes, and the equations reduce to plane-stress regardless of the value of thickness, Δ. Using the 3D submodeling FEM approach described previously, Fig. 3 compares the *ANSYS* result for the stress $\sigma_{zz,\max}$, normalized by far-field stress, σ, with that from
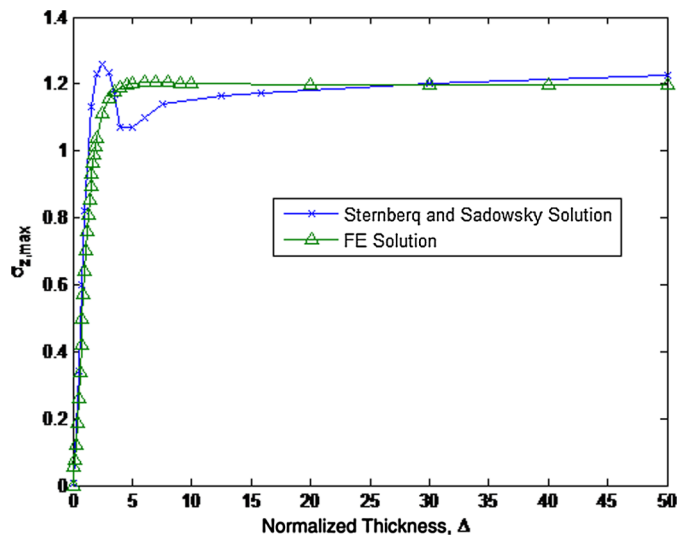

Fig. 3. Analytical (data from Sternberg and Sadowsky 1949) and FEM results for maximum normalized stress in the z-direction in a thick perforated isotropic plate

© ASCE

04016082-3

J. Eng. Mech.

Eq. (10). The agreement between these numerical and analytical results of Fig. 3 further demonstrates the reliability of the present FEM model.

Results for Sitka Spruce

In-Plane Stresses

The variations of $T_x = \sigma_{xx}/\sigma_{yy}$ and stress ratio $\sigma_{yy}(x,0,z)/\sigma_{yy}(a,0,z)$ versus $\zeta = x/a \geq 1$ at $y = 0$ on different vertical perpendicular planes z/L for normalized plate thicknesses $L/a = 5$ are illustrated in Figs. 4 and 5 when the grain direction is parallel to the applied stress, σ. These variations of T_x and $\sigma_{yy}(x,0,z)/\sigma_{yy}(a,0,z)$ for Sitka spruce are similar to those for the isotropic

case (Yang et al. 2008), although the present maximum value of T_x is considerably smaller. Values of T_x and $\sigma_{yy}(x,0,z)/\sigma_{yy}(a,0,z)$ at fixed ζ are virtually insensitive to the different layers, z/L. The present numerically predicted variation of $\sigma_{yy}(x,0,z)/\sigma_{yy}(a,0,z)$ with ζ in Fig. 5 agrees reasonably well with the plane-stress solution of Eq. (5).

If the wood grain orientation is perpendicular to the load, the variations of T_x and $\sigma_{yy}(x,0,z)/\sigma_{yy}(a,0,z)$ versus distances $\zeta = x/a \geq 1$ away from the hole on different planes, z/L, for thickness $L/a = 5$ are shown in Figs. 6 and 7, respectively. The variations of T_x with ζ are now quite different than when the grain direction is parallel to the externally applied stress, σ, or for isotropy (Yang et al. 2008). Fig. 6 shows T_x increased monotonically to reach a relative maximum value. This response is also quite different than in Fig. 4 where values of T_x on the external traction-free surface in
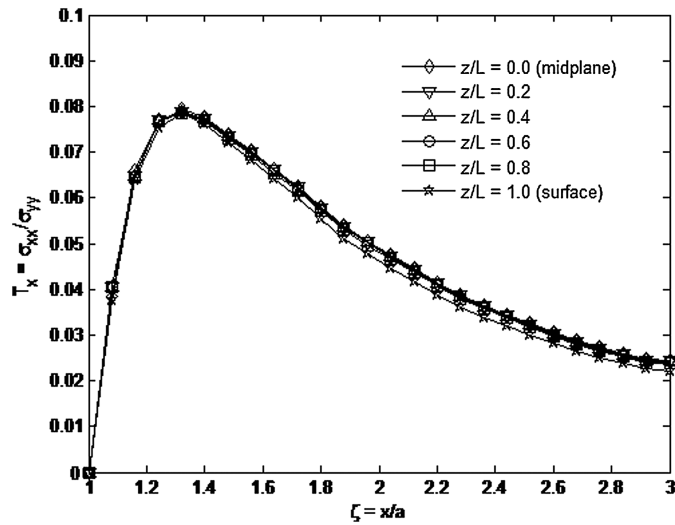

Fig. 4. Variations in stress constraint factor, T_x, for $x/a \geq 1$ on different lateral planes $(x, 0, z/L)$ in Sitka spruce for thickness $L/a = 5$ when longitudinal axis (grain orientation, L-direction) is parallel to applied vertical stress, σ
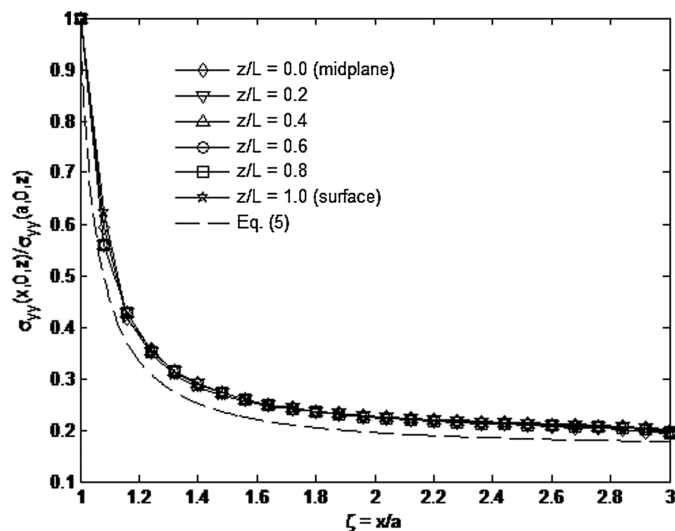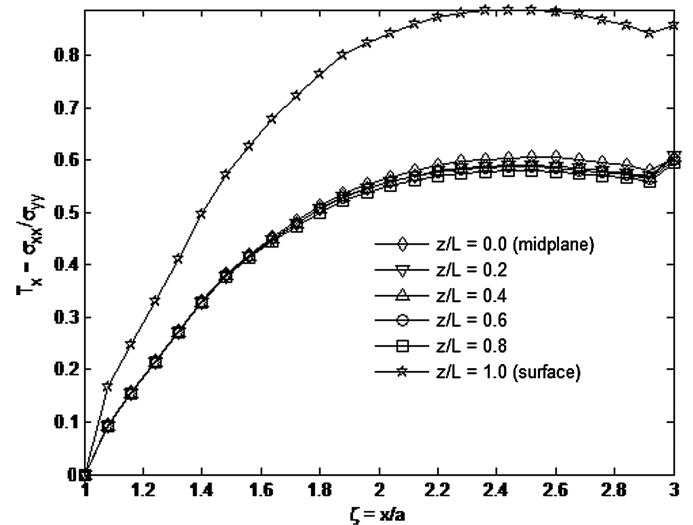

Fig. 6. Variations in stress constraint factor, T_x, for $x/a \geq 1$ on different lateral planes $(x, 0, z/L)$ in Sitka spruce for thickness $L/a = 5$ when longitudinal axis (grain orientation, L-direction) is perpendicular to applied vertical stress, σ

Fig. 5. Variations in stress ratio $\sigma_{yy}(x,0,z)/\sigma_{yy}(a,0,z)$ for $x/a \geq 1$ on different lateral planes $(x, 0, z/L)$ in Sitka spruce for thickness $L/a = 5$ when longitudinal axis (grain orientation, L-direction) is parallel to applied vertical stress, σ

Fig. 7. Variations in stress ratio $\sigma_{yy}(x,0,z)/\sigma_{yy}(a,0,z)$ for $x/a \geq 1$ on different lateral planes $(x, 0, z/L)$ in Sitka spruce for thickness $L/a = 5$ when longitudinal axis (grain orientation, L-direction) is perpendicular to applied vertical stress, σ
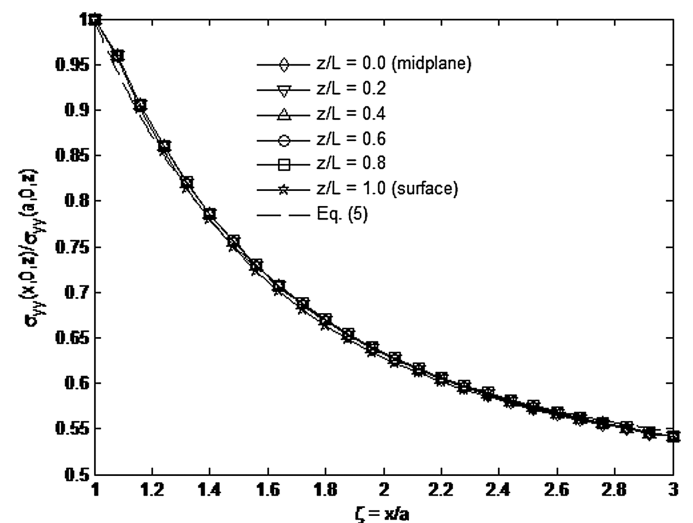
04016082-4

Fig. 6 are much higher than internal values. The plane-stress solution of Eq. (5) and *ANSYS* prediction for $\sigma_{yy}(x, 0, z)/\sigma_{yy}(a, 0, z)$ in Fig. 7 agree with each other.

Distributions of K^σ and K^ε As a Function of Plate Thickness

Figs. 8–11 illustrate the distributions of the stress, K^σ, and strain, K^ε, concentration factors when not and when normalized by the corresponding values at the midplane for different plate thicknesses L/a when the wood grain direction is parallel or perpendicular to the externally applied stress, σ. The stress or strain concentration factors inside the wood plate can exceed those on the external traction-free surfaces by at least 8% (Fig. 8) or 15% (Fig. 9). The biggest differences occurred when $L = a$.
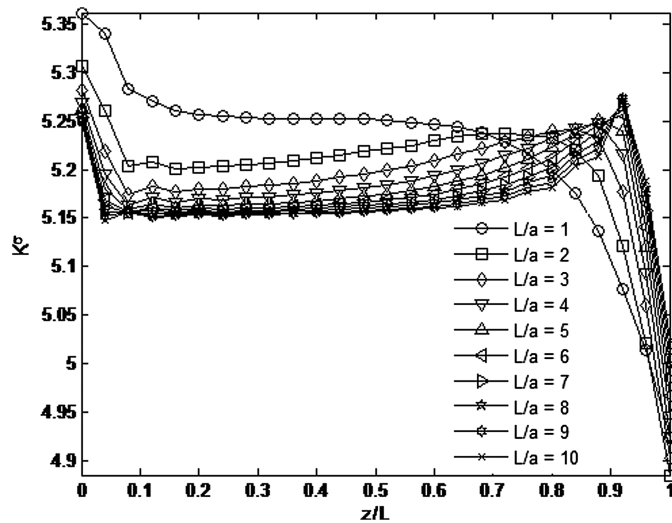
Figs. 10 and 11 illustrate the maximum values of the normalized strain, $K^\varepsilon/K^\varepsilon_{mp}$, concentration factors occur on the midplane ($z/L = 0$) of the spruce plate for small thicknesses L/a (thin plates). As the plate thickness increased, the maximum values occurred on lateral layers close to the external plate surfaces (i.e., $z/L \sim \pm 0.9$). This was not unlike the distributions of K^σ in Fig. 8. When the orientation of the wood grain is parallel to the externally applied stress, the variations of $K^\varepsilon/K^\varepsilon_{mp}$, with respect to changes in thickness L/a, are relatively small in the middle region of the plate (Fig. 10). However, when the wood grain orientation is perpendicular to the externally applied stress, the variation in $K^\varepsilon/K^\varepsilon_{mp}$ increased with respect to changes in thickness (Fig. 11). The plate thicknesses at which the maximum ratios of the strain, $K^\varepsilon/K^\varepsilon_{mp}$, concentration factors shift from midplane to a different plane layer is called the transition thicknesses, L^*_ε, of the strain

Fig. 8. Distribution of stress concentration factors, K^σ, through the thickness in Sitka spruce for different thicknesses when longitudinal axis (grain orientation, L-direction) is parallel to applied vertical stress, σ
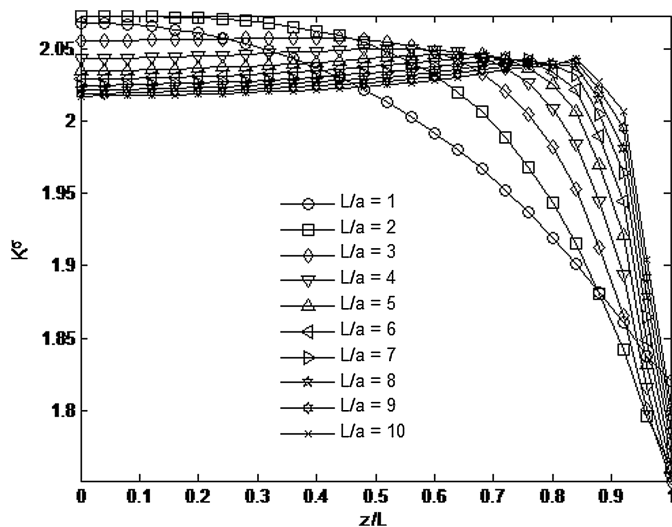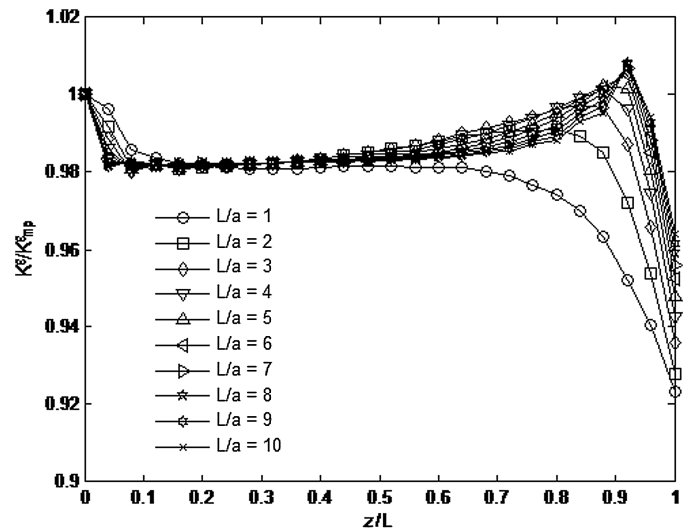

Fig. 10. Distribution of normalized strain concentration factors, $K^\varepsilon/K^\varepsilon_{mp}$, through the thickness in Sitka spruce wood for different thicknesses when longitudinal axis (grain orientation, L-direction) is parallel to applied vertical stress, σ

Fig. 9. Distribution of stress concentration factor, K^σ, through the thickness in Sitka spruce for different thicknesses when longitudinal axis (grain orientation, L-direction) is perpendicular to applied vertical stress, σ

Fig. 11. Distribution of the normalized strain concentration factors, $K^\varepsilon/K^\varepsilon_{mp}$, through the thickness in Sitka spruce for different thicknesses when longitudinal axis (grain orientation, L-direction) is perpendicular to applied vertical stress, σ
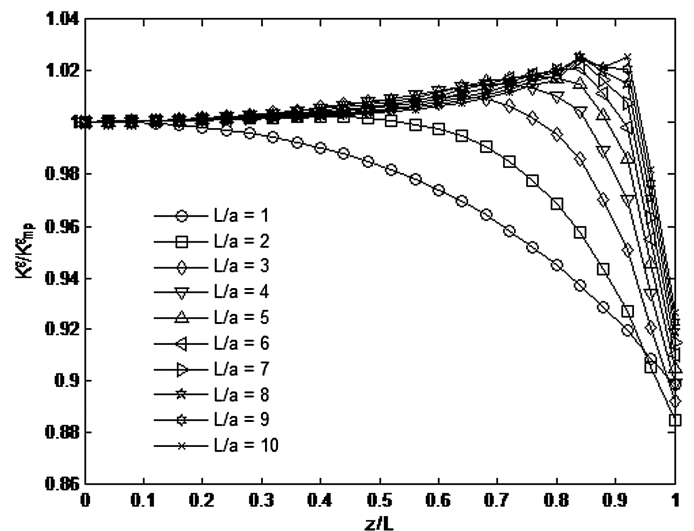
concentration factor. The transition thicknesses, L_ε^*/a, of the strain concentration factor were approximately 4.0 in Fig. 10 and 1.7 in Fig. 11 when the grain direction was parallel and perpendicular to the applied stress, σ, respectively. The maximum values of $K^\varepsilon/K_{mp}^\varepsilon$ increases with increasing plate thickness, L/a. Maximum values of K^σ/K_{mp}^σ and $K^\varepsilon/K_{mp}^\varepsilon$ do not always occur on same plane layer, that is the transition thicknesses of the stress and the strain concentration factor are not equal, $L_\sigma^* \neq L_\varepsilon^*$ (Alshaya 2016). For a thick plate, the transition thickness L_ε^* of the strain concentration factor is smaller than the transition thickness L_σ^* of the stress concentration factor. The Appendix contains some K^σ distributions for a unidirectional graphite/epoxy composite.

Distributions of K_{mp}^σ, K_{mp}^ε, K_{max}^σ, K_{max}^ε, K_{sur}^σ, and K_{sur}^ε As a Function of Plate Thickness

Fig. 12 shows that the distributions of the midplane (K_{mp}^σ and K_{mp}^ε) and maximum (K_{max}^σ and K_{max}^ε) stress and the strain concentration factors normalized by the plane-stress values (K_{ps}^σ and K_{ps}^ε) at the edge of the hole as a function of the spruce plate thickness, L/a. Irrespective of the grain direction, all of these normalized quantities are equal to 1.0 for a very thin plate, i.e., $K_{mp}^\sigma = K_{mp}^\varepsilon = K_{max}^\sigma = K_{max}^\varepsilon = K_{ps}^\sigma$. When the grain direction is perpendicular to the applied stress, σ, $K_{max}^\sigma/K_{ps}^\sigma$ (and $K_{mp}^\sigma/K_{ps}^\sigma$) and $K_{max}^\varepsilon/K_{ps}^\varepsilon$ (and $K_{mp}^\varepsilon/K_{ps}^\varepsilon$) increased to maximum values of 1.06 at $L/a \sim 1.5$ and 1.03 at $L/a \sim 1.0$, respectively. When the grain direction is parallel to the applied stress, the values of all of these ratios initially increased slightly and thereafter decreased to individual constant values as L/a increases.

Fig. 12 also illustrates that when $K_{max}^\sigma/K_{ps}^\sigma$ separates from $K_{mp}^\sigma/K_{ps}^\sigma$, the transition thicknesses, L_σ^*, of the stress concentration factor are located at $L/a = 7.0$ and 3.0, and when $K_{max}^\varepsilon/K_{ps}^\varepsilon$ separated from $K_{mp}^\varepsilon/K_{ps}^\varepsilon$, the transition thickness, L_ε^*, of strain concentration factor was located at $L/a = 4.0$ and 1.7 when the grain direction is parallel and perpendicular to the applied stress, σ, respectively. The values of $K_{max}^\sigma/K_{ps}^\sigma$ exceeded those for $K_{max}^\varepsilon/K_{ps}^\varepsilon$. The values of $K_{max}^\sigma/K_{ps}^\sigma$ and $K_{max}^\varepsilon/K_{ps}^\varepsilon$ are greater when the grain

orientation is perpendicular to the load than if they were parallel to each other.

Fig. 13 demonstrates that the values of stress K_{sur}^σ and strain K_{sur}^ε concentration factors at the traction-free surfaces of the plate are equal (although equal to different values depending whether the grain is parallel or perpendicular to the externally applied stress) for all the thicknesses. When the grain orientation parallels the applied stress, σ, the surface stress K_{sur}^σ and strain K_{sur}^ε concentration factors reached a minimum value of $(K_{sur}^\sigma/K_{ps}^\sigma)_{min} \sim 0.9$ at $L/a = 1.8$, then increased gradually as the normalized thickness increased.

Fig. 14 shows the differences between the midplane (K_{mp}^σ and K_{mp}^ε) or the maximum (K_{max}^σ and K_{max}^ε) stress and strain

Fig. 13. Distributions of normalized external traction-free surface stress, $K_{sur}^\sigma/K_{ps}^\sigma$, and strain, $K_{sur}^\varepsilon/K_{ps}^\varepsilon$, concentration factors in Sitka spruce as function of plate thickness L/a for different rain orientations (parallel—solid line and perpendicular—dashed line) to applied vertical stress, σ
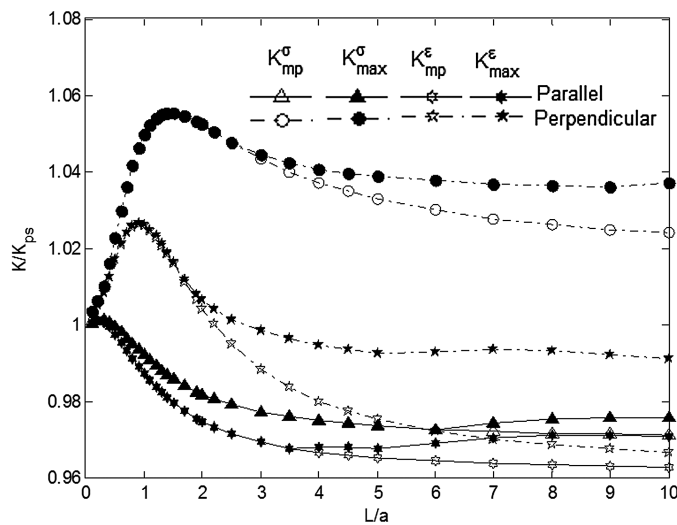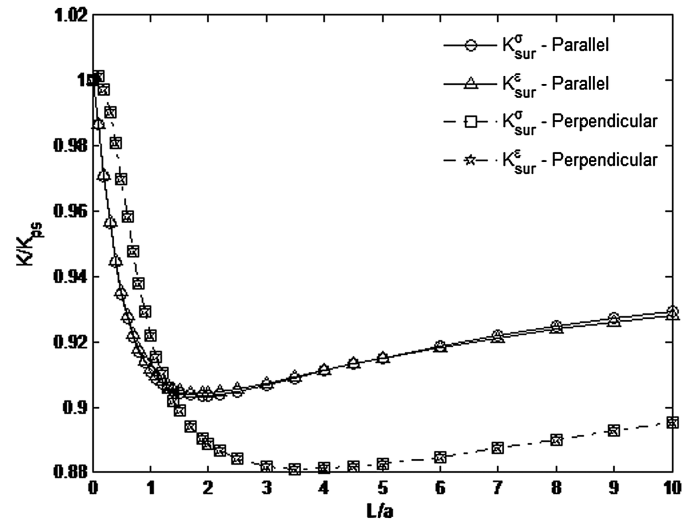

Fig. 12. Distributions of normalized midplane ($K_{mp}^\sigma/K_{ps}^\sigma$ and $K_{mp}^\varepsilon/K_{ps}^\varepsilon$) and maximum ($K_{max}^\sigma/K_{ps}^\sigma$ and $K_{max}^\varepsilon/K_{ps}^\varepsilon$) stress and strain concentration factors in Sitka Spruce as function of plate thickness L/a for different grain orientations (parallel—solid line and perpendicular—dashed line) to applied vertical stress, σ
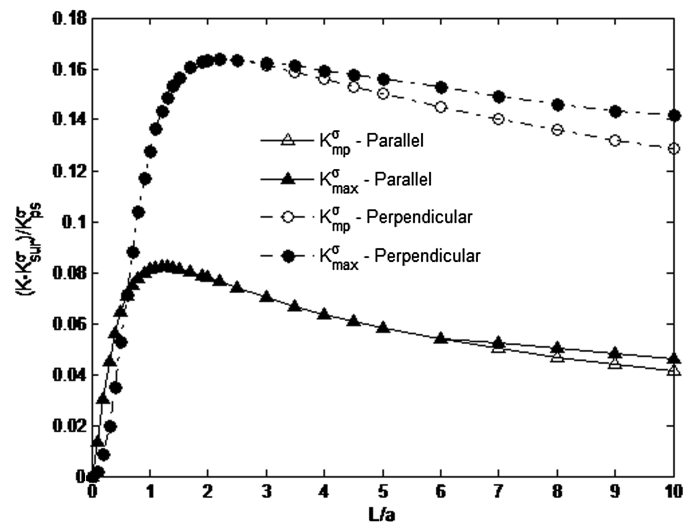

Fig. 14. Differences between the normalized midplane, $(K_{mp}^\sigma - K_{sur}^\sigma)/K_{ps}^\sigma$, and maximum, $(K_{max}^\sigma - K_{sur}^\sigma)/K_{ps}^\sigma$ and surface stress concentration factors in Sitka spruce as a function of normalized plate thickness L/a when the grain orientation is parallel and perpendicular to applied vertical stress, σ

concentration factors and the plate's surface values (K_{sur}^{σ} and K_{sur}^{ε}) normalized by the plane stress-state values (K_{ps}^{σ} and K_{ps}^{ε}) versus L/a for different grain orientations. The difference between midplane K_{mp}^{σ} (or maximum K_{max}^{σ}) and surface K_{sur}^{σ} stress concentration factor increased with increasing thickness L/a until reaching a maximum value of approximately 8% and 16% of the plane-stress value when the grain orientation is parallel or perpendicular to the vertically applied stress, σ, respectively (Fig. 14). After reaching their maximum values, these quantities decreased gradually as thickness, L/a, increased.

Fig. 15 illustrates trends similar to those in Fig. 14, although the largest difference between the maximum and surface stress concentration factors (Fig. 14) exceeds the maximum difference between the midplane and surface strain concentration factors (Fig. 15). The difference between midplane K_{mp}^{ε} and surface K_{sur}^{ε} strain concentration factor increased with increasing thickness L/a until reaching maximum values of approximately 8% and 12% of the plane-stress value when the grain orientation is parallel and perpendicular to the vertically applied stress, σ, respectively. After reaching their maximum values, all curves of Figs. 14 and 15 decreased gradually with increasing thickness, L/a. Fig. 15 shows that measured strains on the plate surface can be 12% less than at midplane.

Relationship between Stress and Strain Concentration Factors

For an orthotropic plate, the relationship between the stress and strain concentration factors can be expressed by Eq. (7). Figs. 8–11 show that the distributions of stress concentration factors are different from strain concentration factors through the thickness of the plate. For a finite thickness orthotropic plate, the ratio of the stress and strain concentration factor, $K^{\varepsilon}/K^{\sigma}$, is a function of Poisson's ratios ν_{yx} and ν_{yz} and the in-plane T_x and out-of-plane T_z stress constraint factors [Eq. (7)]. Since $T_x = 0$ for $(a, 0, z)$ and $T_z = 0$ at the midplane $(z/L = 0)$ and on the external surfaces $(a, 0, \pm L)$, the stress and strain concentration factors are equal, $K^{\varepsilon} = K^{\sigma}$ at $(a, 0, \pm L)$. This is compatible with results in Fig. 13. However, $T_x \neq 0$ when $x/a > 1$ and $T_z \neq 0$ if
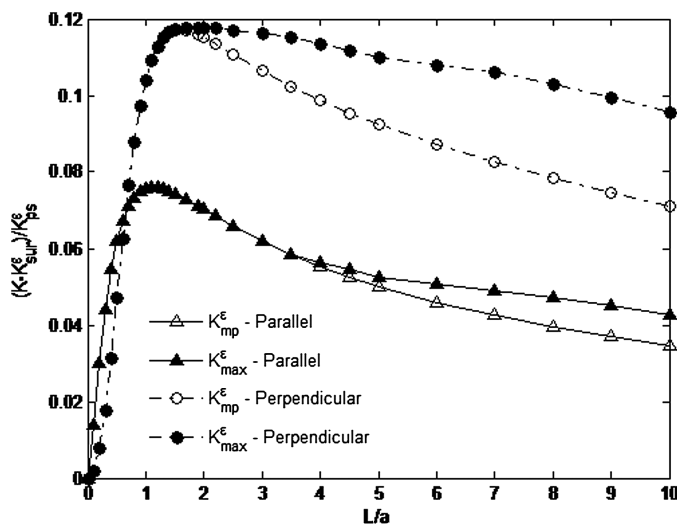
$0 < z/L < \pm 1$, so $K^{\varepsilon} \neq K^{\sigma}$ when $x/a > 1$ and $0 < z/L < \pm 1$, these features are substantiated in Figs. 16 and 17. The distributions of $K^{\varepsilon}/K^{\sigma}$ within the thickness, $0 < z/L < \pm 1$ at $x/a = 1$ and $y = 0$ is a function of the Poisson's ratio, ν_{yz}, and out-of-plane stress constraint factors ($T_x = 0$, $T_z \neq 0$). On the other hand, the distributions of $K^{\varepsilon}/K^{\sigma}$ at $x/a \geq 1$ on the external surfaces of the plate, $y = 0$ and $z = \pm L$, are a function of the Poisson ratio, ν_{yx}, and the in-plane stress constraint factor ($T_z = 0$).

Distribution of $K^{\varepsilon}/K^{\sigma}$ for $x/a \geq 1$ for Different Plane Layers

Figs. 16 and 17 show the distributions of $K^{\varepsilon}/K^{\sigma}$ at $x/a \geq 1$, $y = 0$ for different lateral planes parallel to the midplane of the plate for $L/a = 1$ and 5 when the grain orientation is parallel to the applied stress. These distributions are different on different planes. Each curve corresponding to its plane has a minimum value and location
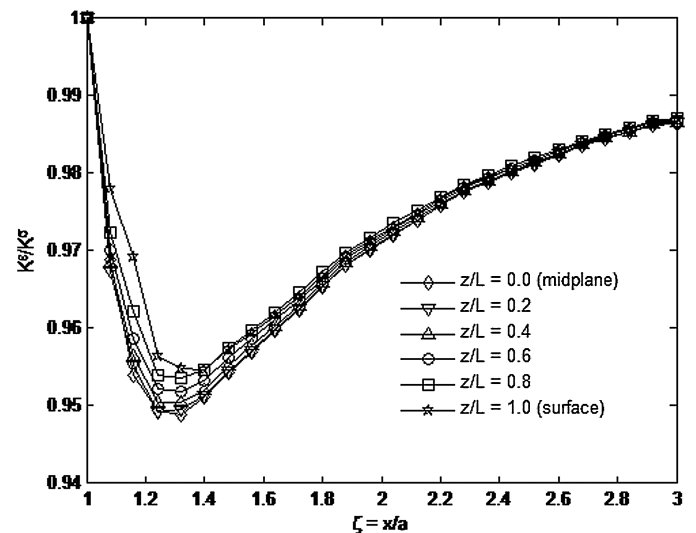

Fig. 16. Distributions of $K^{\varepsilon}/K^{\sigma}$ in Sitka spruce on different planes for $L/a = 1$ when longitudinal axis (grain orientation, L-direction) is parallel to applied vertical stress, σ

Fig. 15. Differences between the normalized midplane, $(K_{mp}^{\varepsilon} - K_{sur}^{\varepsilon})/K_{ps}^{\varepsilon}$, and maximum, $(K_{max}^{\varepsilon} - K_{sur}^{\varepsilon})/K_{ps}^{\varepsilon}$, and surface stress concentration factors in Sitka spruce as a function of normalized plate thickness L/a when the grain orientation is parallel or perpendicular to applied vertical stress, σ

Fig. 17. Distributions of $K^{\varepsilon}/K^{\sigma}$ in Sitka spruce on different planes for $L/a = 5$ when longitudinal axis (grain orientation, L-direction) is parallel to applied vertical stress, σ
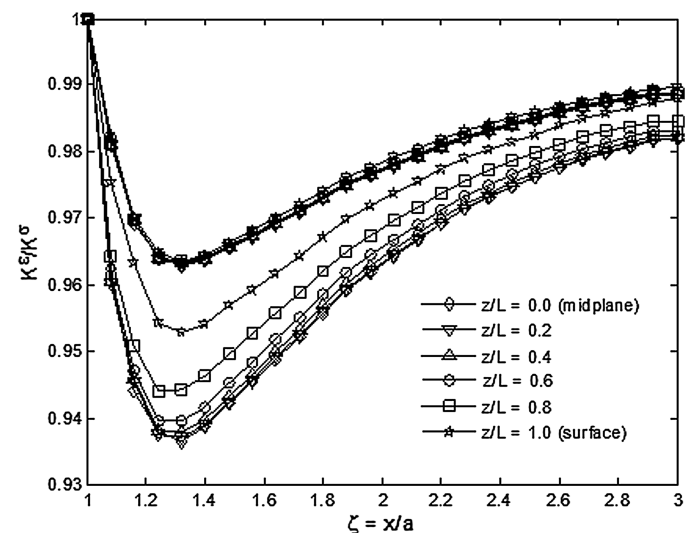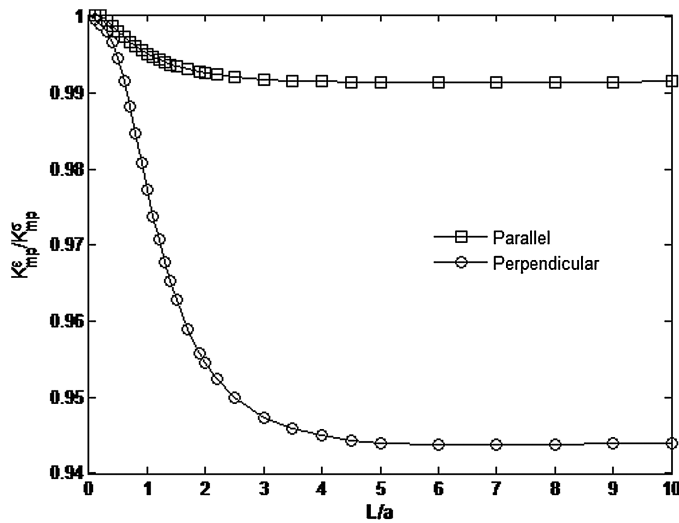
Fig. 18. Distribution of midplane K^ε/K^σ at the edge of the hole in Sitka spruce as a function of thickness when the grain orientation is parallel or perpendicular to applied vertical stress, σ

which depends on Poisson's ratios, the plane's location, and the thickness of the plate. All curves start at $K^\varepsilon/K^\sigma = 1.0$ on the edge of the hole ($\zeta = 1.0$), decrease for $\zeta \geq 0$ (i.e., $T_x \neq 0$) and pass through minimum values at approximately at $\zeta = 1.3$. These minimum values increase as one moves from the external surfaces ($z/L = \pm 1$) toward the center of the plate ($z/L = 0$).

Distribution of K^ε/K^σ along the Edge of the Hole for Different Thicknesses

The distributions of K^ε/K^σ along the edge of the hole and through the thickness for different normalized thicknesses and different grain orientations were obtained, and the minimum values through the thickness of the edge of the hole occur on the midplane layer. This minimum value decreased with the increasing normalized thickness (Alshaya 2016).

Distribution of Midplane Values of K^ε/K^σ As a Function of Thickness

Fig. 18 shows the distribution of midplane values of $K^\varepsilon_{\mathrm{mp}}/K^\sigma_{\mathrm{mp}}$ as a function of plate thickness when the grain orientation is parallel or perpendicular to the applied stress, σ. Starting at $K^\sigma_{\mathrm{mp}} = 1$, plane-stress (i.e., $L/a \sim 0$), these curves decreased monotonically with increasing thickness until $L/a > \sim 4$ where they approached constant (but different) values. The magnitudes of $K^\varepsilon_{\mathrm{mp}}/K^\sigma_{\mathrm{mp}}$ for very thick plates are substantially greater when the grain orientation of the wood is parallel, rather than perpendicular, to the externally applied stress, σ.

Summary, Discussion, and Conclusions

1. Not unlike in isotropic plates (Yang et al. 2008), the stress and/or strain concentrations in perforated loaded orthotropic plates depend on the relative plate thickness. However, many results under orthotropy can be quite different from those in isotropic plates. In particular, they depend on whether the strongest/stiffest principal material direction is parallel or perpendicular to the direction of the external loading.
2. Figs. 4–7 show that the distributions of $\sigma_{yy}(x,0,z)/\sigma_{yy}(a,0,z)$, are similar for isotropic (Yang et al. 2008) and

orthotropic Sitka spruce plates when the vertical applied stress, σ, is either parallel or perpendicular to the grain orientation. However, the distribution of T_x for an orthotropic plate when the applied stress, σ, is perpendicular to the grain can be different than when the applied stress, σ, is parallel to the grain or for an isotropic material. When the wood grain orientation is parallel to the applied loading, the maximum stress concentration factor occurs on the midplane and exceeds that on the external traction-free surface by ∼8% (Fig. 8). When the wood grain is perpendicular to the applied loading (Fig. 9), the maximum stress concentration factor again occurs on the midplane and is ∼15% higher than that on the external surface. By comparison, Sternberg and Sadowsky (1949) showed that for an isotopic plate whose thickness is 0.7 that of the radius of the hole, the maximum stress concentration factor at the traction-free surface is 7% less, whereas that at the midplane is 3% higher, than the plane-stress value. Even when all other things are equal, unlike with isotropy, the stresses in orthotropic materials depend on the constitutive properties.
3. Irrespective of whether or not they are normalized, the through-thickness distributions of the stress or strain concentration factors (K^σ or K^ε) depend on the plate thickness (Figs. 8–11). The maximum $K^\sigma_{\mathrm{max}}/K^\sigma_{\mathrm{mp}}$ and $K^\varepsilon_{\mathrm{max}}/K^\varepsilon_{\mathrm{mp}}$ at the edge of the hole occur at the midplane ($z/L = 0$) for relatively thin plates but on various planes close to (but not at) the plate's external traction-free surfaces for thick plates.
4. For the present Sitka spruce material, for thicker plates, the stress and strain concentration factors decrease rapidly near the external traction-free surfaces ($z/L = \pm 1$) and reach lower values that are not representative of the overall stress and strain concentration factors through thickness (Figs. 8–11). The stress or strain concentrations on the midplane can increase from their plane-stress values when $L/a = 1$ to some relative maximum in a thicker plate and then decrease in much thicker plates (Fig. 12).
5. The normalized stress and strain concentration factors ($K^\sigma_{\mathrm{sur}}/K^\sigma_{\mathrm{mp}}$ and $K^\varepsilon_{\mathrm{sur}}/K^\varepsilon_{\mathrm{mp}}$) at the edge of the hole are essentially equal to each other and decrease with the increasing plate thickness (Fig. 13).
6. Since the tensile strength transverse to the wood grain or the fibers in structural orthotropic composites is usually appreciably less than that parallel to the grain or fibers, the present results can be particularly significant. For a plate is loaded in tension, the structural strength can be very low when the wood grain is perpendicular to the direction of externally applied stress. On the other hand, the low tensile strength perpendicular to the strong/stiff material direction in orthotropic composites can be particularly detrimental in tensile-loaded bolted joints involving such materials in that it often leads to splitting of the material supporting the bolt. Recognizing that the worst stresses in thick plates frequently occur subsurface, such splitting could initiate below the surface and hence not be detected prior to catastrophic structural failure.
7. The distributions of K^ε/K^σ for $x/a \geq 1$ (away from the hole) are different on different planes and each curve corresponding to its plane has a minimum whose value depends on the Poisson's ratios, plane-location, and the plate thickness (Fig. 16). Although the present minimums in the Sitka spruce tend to occur at a common location away from the hole, the minimum locations might depend on material properties.
8. The directional strength dependency, combined with the fact that stresses σ_x, σ_y, and σ_z can all be nonzero on internal planes ahead of the hole (i.e., $x/a \geq 1$), can be a strength concern in orthotropic materials.

**Table 2.** Constitutive Properties of Unidirectional Carbon/Epoxy Composite (Data from Daniel and Ishai 2006)

Property	Value
Elastic moduli (GPa)	
E_{11}	147
E_{22}	10.3
E_{33}	10.3
Shear moduli (GPa)	
G_{12}	7.0
G_{23}	3.7
G_{13}	7.0
Poisson's ratios	
ν_{12}	0.27
ν_{23}	0.54
ν_{13}	0.27
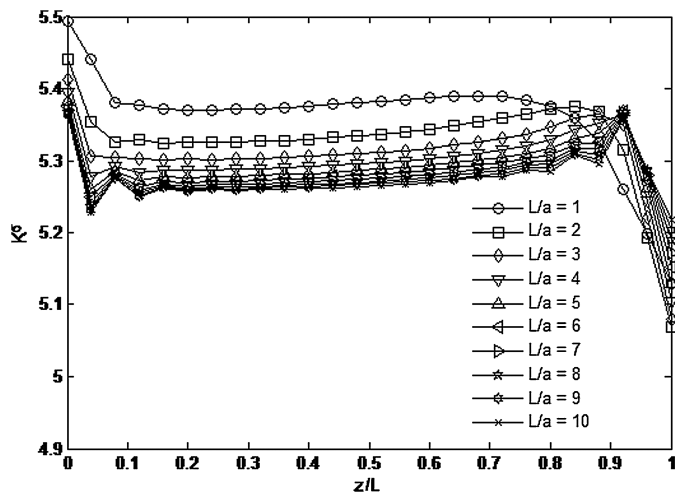
Fig. 19. Distribution of normalized stress concentration factors, K^σ, through the thickness in carbon/epoxy for different thicknesses when the one-direction is parallel to applied vertical stress, σ

9. That maximum stresses and/or strains associated with holes can occur other than on the external traction-free plate surfaces where measurements are most readily made is technically significant.
10. The stress and strain concentrations factors are equal to each other only at the edge of the hole.
11. This manuscript emphasizes the response in a highly orthotropic structural material, Sitka spruce. However, the Appendix contains some comparative results for a unidirectional carbon-epoxy composite. As with the Sitka spruce, the maximum stress concentrations in such artificial composites can occur below the external surfaces.
12. The principal material directions are aligned here with the plate geometry and loading. Consideration should be given to cases when the principal material directions are inclined to the plate geometry and direction of loading.

Appendix. Results for Carbon/Epoxy Composite

For the geometry and loading of Fig. 1, and elastic properties of Table 2, Figs. 19 and 20 show the distributions of the stress concentration factors, K^σ, as a function plate thicknesses in a carbon/epoxy plate when the strong/stiff orientation (one-direction) is
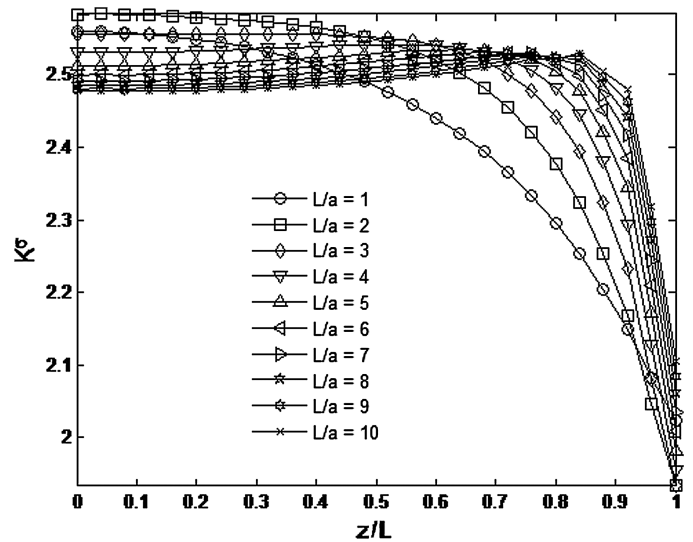
Fig. 20. Distribution of normalized stress concentration factors, K^σ, through the thickness in carbon/epoxy for different thicknesses when two-direction is parallel to applied vertical stress, σ

parallel or perpendicular to the externally applied stress. These results were obtained using the same *ANSYS* modeling as for wood. The present trends are not unlike those for the Sitka spruce (Figs. 8 and 9). The plane-stress stress concentrations the edge of a round hole in an infinite orthotropic plate is given by Lekhnitskii (1969)

$$K^\sigma = 1 + \mathrm{Re}\left(i \frac{\mu_1 + \mu_2}{\mu_1 \mu_2} \right) \tag{11}$$

For the carbon/epoxy, Eq. (11) gives 5.57 and 2.40 for the load parallel and perpendicular to strong/stiff orientation, whereas Figs. 19 and 20 give 5.5 and 2.56 at $L/a = 1$, respectively. When the longitudinal axis (grain orientation, *L*-direction) in the Sitka spruce is parallel and perpendicular to the applied vertical stress, σ, Eq. (11) gives 5.99 and 2.0, respectively. For a thin plate (plane stress), Figs. 8 and 9 give 5.35 and 2.08, respectively, at $L/a = 1$.

Acknowledgments

References

Alshaya, A. (2016). "Experimental, analytical and numerical analyses of orthotropic materials." Ph.D. thesis, Univ. of Wisconsin-Madison, Madison, WI.

ANSYS [Computer software]. ANSYS, Canonsburg, PA.

Broek, D. (1987). *Elementary engineering fracture mechanics*, Kluwer Academic Press, Hingham, MA.

Dai, L., and Gong, J. (2013). "The three-dimensional stress field in an arbitrary thickness plate holding a circular hole." *Int. J. Mech. Syst. Eng.*, 3(2), 75–82.

Daniel, I. M., and Ishai, O. (2006). *Engineering mechanics of composite materials*, 2nd Ed., Oxford University Press, New York.

Folias, E. S. (1975). "On the three-dimensional theory of cracked plates." *J. Appl. Mech.*, 42(3), 663–674.

Folias, E. S. (1987). "The 3D stress field at the intersection of a hole and a free surface." *Int. J. Fract.*, 35(3), 187–194.

Folias, E. S., and Wang, C. H. (1990). "On the three-dimensional stress field around a circular hole in a plate with arbitrary thickness." *J. Comput. Mech.*, 6(5–6), 379–391.

Kotousov, A., and Tan, P. J. (2004). "Effect of the plate thickness on the out-of-plane displacement field of a cracked elastic plate loaded in mode I." *Int. J. Fract.*, 127(1), L97–L103.

Kotousov, A., and Wang, C. H. (2002a). "Fundamental solutions for the generalized plane strain theory." *Int. J. Eng. Sci.*, 40(15), 1775–1790.

Kotousov, A., and Wang, C. H. (2002b). "Three-dimensional solutions for transversally isotropic plates." *J. Compos. Struct.*, 57(1–4), 445–452.

Kotousov, A., and Wang, C. H. (2002c). "Three-dimensional stress constraint in an elastic plate with a notch." *Int. J. Solids Struct.*, 39(16), 4311–4326.

Lekhnitskii, S. G. (1969). *Theory for elasticity of an anisotropic body*, Holden-Day, San Francisco.

Pilkey, W. D., and Pilkey, D. F. (2008). *Peterson's stress concentration factors*, Wiley, New York.

Rhee, J., Cho, H. K., Marr, R. J., and Rowlands, R. E. (2012). "Local compliance, stress concentrations and strength in orthotropic materials." *J. Stress Anal. Eng. Des.*, 47(2), 113–128.

Sternberg, E., and Sadowsky, M. A. (1949). "Three-dimensional solution of the stress concentration around a circular hole in a plate with arbitrary thickness." *J. Appl. Mech.*, 16(1), 27–38.

Timoshenko, S., and Goodier, J. N. (1970). *Theory of elasticity*, McGraw-Hill, New York.

Wood Handbook–Wood as an Engineering Material. (1999). "General technique report FPL-GTR-113." U.S. Dept. of Agriculture, Forest Service, Forest Products Laboratory, Madison, WI.

Yang, Z., Kim, C. B., Cho, C., and Beom, H. G. (2008). "The concentration of stress and strain in finite thickness elastic plate containing a circular hole." *Int. J. Solids Struct.*, 45(3–4), 713–731.

Young, W. C., and Budynas, R. G. (2002). *Roark's formulas for stress and strain*, 7th Ed., McGraw Hill, New York.

Youngdal, C. K., and Sternberg, E. (1966). "Three-dimensional stress concentrations around a cylindrical hole in a semi-infinite elastic body." *J. Appl. Mech.*, 33(4), 855–865.